Novel Splice Donor Site Mutation in the Cardiac Myosin-binding Protein-C Gene in Familial Hypertrophic Cardiomyopathy

Characterization of Cardiac Transcript and Protein

Wolfgang Rottbauer,* Mathias Gautel,‡ Jörg Zehelein,* Siegfried Labeit,‡ Wolfgang M. Franz,§ Christine Fischer,‖ Benedikt Vollrath,* Gerhard Mall,¶ Reiner Dietz, Wolfgang Kübler,* and Hugo A. Katus§**

**Medizinische Klinik III, Universität Heidelberg, D-69115 Heidelberg, Germany; ‡European Molecular Biology Laboratory, D-69012 Heidelberg; §Medizinische Klinik II, Universität zu Lübeck, D-23562 Lübeck, Germany; ‖Institut für Humangenetik, Universität Heidelberg, D-69120 Heidelberg; ¶Pathologisches Institut, Städtische Kliniken Darmstadt, D-64283 Darmstadt, Germany; and **Franz-Volhard Klinik und Max-Delbrück Centrum, D-13125 Berlin, Germany*

Abstract

Familial hypertrophic cardiomyopathy is a disease generally believed to be caused by mutations in sarcomeric proteins. In a family with hypertrophic cardiomyopathy linked to polymorphic markers on chromosome 11, we found a new mutation of a splice donor site of the cardiac myosin-binding protein-C gene. This mutation causes the skipping of the associated exon in mRNA from lymphocytes and myocardium. Skipping of the exon with a consecutive reading frame shift leads to premature termination of translation and is thus expected to produce a truncated cardiac myosin-binding protein-C with loss of the myosin- and titin-binding COOH terminus. However, Western blot analysis of endomyocardial biopsies from histologically affected left ventricular myocardium failed to show the expected truncated protein.

These data show for the first time that a splice donor site mutation in the myosin-binding protein-C gene is transcribed to cardiac mRNA. Truncated cardiac myosin-binding protein-C does not act as a "poison polypeptide," since it seems not to be incorporated into the sarcomere in significant amounts. The absence of mutant protein and of significantly reduced amounts of wild-type protein in the presence of the mutated mRNA argues against the "poison protein" and the "null allele" hypotheses and suggests yet unknown mechanisms relevant to the genesis of chromosome-11–associated familial hypertrophic cardiomyopathy. (*J. Clin. Invest*. 1997. 100:475–482.) Key words: cardiac myosin-binding protein-C • myocardial tissue • null allele • sarcomere assembly • cotranslation

Introduction

Familial hypertrophic cardiomyopathy (FHC)[1] is inherited as an autosomal dominant disease that is characterized by unexplained cardiac hypertrophy (1). Previous genetic analyses have shown positive linkage to five different loci and four disease genes have been identified: β-myosin heavy-chain (2, 3), α-tropomyosin (4, 5), cardiac troponin T (5, 6), and, recently, cardiac myosin-binding protein-C (MyBP-C) on chromosome 11p13-q13 (7–9). The disease gene for the chromosome-7 associated form of FHC is still unknown (10). Based on altered lymphocyte cDNA, the thus far described mutations of MyBP-C are predicted to produce a truncated cardiac protein with disruption of the titin and myosin-binding COOH-terminal region. At present, it is unknown whether these mutations are also expressed in myocardium. We now describe a family with FHC and a novel MyBP-C splice donor site mutation, in which endomyocardial biopsy specimens of the index patient were available for RNA and protein analysis.

Methods

Index family. Since 1988, the clinical characteristics and blood samples of all patients with cardiomyopathy are collected in a registry at the University Hospital of Heidelberg (Heidelberg, Germany). 51 patients were classified as having FHC. DNA from blood lymphocytes of these patients was screened by single strand conformation polymorphism (SSCP) analysis for mutations in candidate genes including cardiac MyBP-C. In one patient, a band shift in cardiac MyBP-C was observed on SSCP. This index patient and his core family represent the study group.

A detailed history was obtained by interviewing the index patient and his sons. Members of the family who live in Turkey were not available for clinical investigation. All members of the core family underwent a physical examination, clinical chemistry testing, a 12-lead electrocardiogram recording, and an echocardiographic study. The diagnostic criteria for hypertrophic cardiomyopathy were defined as unexplained hypertrophy of left ventricular myocardium, which was assessed by M-mode echocardiographic measurements using the diagnostic criteria of the American Society of Echocardiography (11–13). Left and right heart catheterization and coronary angiography were performed in the index patient at baseline and at a 1-yr follow up. Left ventricular wall thickness was assessed in 30° left anterior oblique projection by simultaneous injection of 30 ml contrast material in both ventricular chambers. Six ventricular biopsies were taken from the interventricular septum at baseline and at the 1-yr follow up. The study protocol was approved by the ethics committee on human research of the University of Heidelberg, and all participants gave informed consent after a thorough explanation of the study protocol.

Address correspondence to Hugo A. Katus, Medizinische Klinik II, University of Lübeck, Ratzeburger Allee 160, 23562 Lübeck, Germany. Phone: 49-451-5002500; FAX: 49-451-5006437; E-mail: Rattbaue@medinf.mu-luebeck.de

Received for publication 21 August 1996 and accepted in revised form 17 April 1997.

J. Clin. Invest.

0021-9738/97/07/0475/08 $2.00
Volume 100, Number 2, July 1997, 475–482

1. *Abbreviations used in this paper:* FHC, familial hypertrophic cardiomyopathy; MyBP-C, myosin-binding protein-C; SSCP, single strand conformation polymorphism.

Genotype analysis. Microsatellite markers derived from the genetic map of Gyapay et al. (14) were analyzed using the PCR conditions and multiplex procedure described by Vignal (15). PCR products were resolved according to size by polyacrylamide gel electrophoresis as described below and detected by silver staining.

Linkage analysis. Calculations of possible linkage by the computer program MLINK (16) were performed with affection status as indicated in Fig. 1 (below) and disease penetrance of 90%. Linkage was tested for β-myosin (MYO I, MYO II), α-tropomyosin (D15S108, D15S114), cardiac troponin T (D1S202, D1S412), and cardiac MyBP-C genes (D11S1344, D11S1350, novel splice donor site mutation). The allele frequency for the G→A transversion in the cardiac MyBP-C gene was estimated at 0.02 based on its absence from 250 normal chromosomes (upper limit of the 95% binomial confidence interval of 0/250).

DNA and RNA isolation from peripheral blood lymphocytes. Genomic DNA was extracted from blood samples of all family members using the genomic DNA extraction kit (Qiagen, Hilden, Germany) in accordance with manufacturer's protocol.

mRNA was extracted from peripheral lymphocytes, isolated from whole blood over a Ficoll-Paque Plus (Pharmacia LKB Biotechnology, Uppsala, Sweden) gradient with the Oligotex™ Direct mRNA MidiKit (Qiagen).

RNA extraction from myocardial biopsies. Total RNA was isolated from endomyocardial biopsies of left ventricular myocardium according to the method described by Chirgwin et al. (17).

Cardiac MyBP-C oligonucleotides. All nucleotides were 20mers synthesized according to the published cDNA sequence (18) and numbered according to the position of the 5′ residue. F indicates forward and R reverse orientation.

Amplification of cDNA sequences. 0.2 μg RNA obtained from lymphocytes or myocardial tissue was reverse transcribed in a 20-μl volume as follows; 4 μl of reverse transcription buffer, 2 μl of 0.1 M DTT, 0.25 μl of RNA Guard, and 10 U H-Reverse Transcriptase Superscript from GIBCO BRL, Life Technologies (Eggenstein, Germany), 1 μl of 10 μM pd(N_6)-primer, and 1 μl of 1 mM dNTP from Pharmacia LKB Biotechnology were added to preheated (68°C, 5 min) RNA in a total volume of 20 μl. The reaction was incubated at 37°C for 1 h and terminated by heat inactivation (95°C, 5 min).

The cDNA products were then amplified in a 50-μl PCR reaction using the outer primer pair 2968F and 3729R. The second round of PCR was performed with a 1:100 final dilution of the first round products and the primer 3300F and the 5′-fluorescein–labeled primer 3566R (Pharmacia LKB Biotechnology). The amplification was performed as follows: 0.5 μl of the reverse transcription product was added to 50 μl of PCR mix. The PCR reaction mix contained 25 pM of each primer, 200 μM 4-dNTP (Pharmacia LKB Biotechnology), 1 U Thermus aquaticus DNA polymerase (Pharmacia LKB Biotechnology), 10 mM Tris-HCL, pH 8.3, at room temperature, 50 mM KCl, and 1.5 mM $MgCl_2$. The PCR reaction was denatured by a 92.5°C incubation for 3 min, and then amplified for 20, 25, 30, 35, 40, and 45 cycles in a Hybaid Omnigene Temperature Cycler (Hybaid Ltd., Teddington, UK). Each cycle consisted of denaturing at 92.5°C for 50 s, annealing at 55°C for 50 s, and extension at 72°C for 60 s.

Semiquantitation of cDNA products. PCR products were loaded onto 5–15% polyacrylamide gradient gels (2,350 × 1,500 mm). The products were separated on a Multiphor II Electrophoresis System (Pharmacia LKB Biotechnology) by 60 mA for 2 h at 20°C and transferred to a nylon membrane (Biodyne A Transfer Membrane; BioSupport Division Pall Filtrationstechnik, Dreieich, Germany) essentially as described (19). PCR products were visualized with the ECL-system following the instructions of the supplier (Amersham Life Sciences, Braunschweig, Germany). Blots were exposed on hyperfilm-MP (American Life Sciences) between 20 s and 5 min. The ratio of the mutant to the wild-type allele was determined by densitometrical scanning of the films (20).

Genomic DNA amplification. The primer pairs 3300F–3490R and 3445F–3576R were used to amplify the region of interest. The PCR reaction mix contained 75 ng DNA as the template, 25 pM of each primer, 200 μM 4-dNTP, 1 U Thermus aquaticus DNA polymerase, 10 mM Tris-HCL, pH 8.3, at room temperature, 50 mM KCL, and 1.5 mM $MgCl_2$ in a volume of 50 μl. The DNA was denatured by exposing it to 92.5°C for 3 min, and then amplified for 30 cycles in a Hybaid Omnigene Temperature Cycler. Each cycle consisted of a denaturation step at 92.5°C for 50 s, an annealing step at 60°C for 50 s, and an extension step at 72°C for 60 s.

Single strand conformation polymorphism analysis. PCR products were denatured by adding 7 μl of 95% formamide to 7 μl of the PCR product followed by heating for 5 min at 92.5°C. The solution was then chilled on ice for 10 min, loaded onto 5–15% polyacrylamide gradient gels (2,350 × 1,500 mm). The products were separated on a Multiphor II Electrophoresis System by 60 mA for 2 h at 20°C and visualized by silver staining (21).

BstnI endonuclease digest. 12 μl of the PCR product was digested for 3 h at 60°C by 2 U of the restriction enzyme BstnI (New England Biolabs Inc., Beverly, MA) in 25 μl with addition of the appropriate buffer and 0.1 μg BSA. Fragments were resolved by electrophoresis on 5–15% polyacrylamide gels as outlined above and visualized by silver staining.

Cloning of PCR products. DNA and cDNA sequences were confirmed by subcloning in a pBluescript II KS (+/−) phagemid vector (Stratagene Inc., Heidelberg, Germany). Recombinant plasmid DNA was purified by the alkaline lysis method (Plasmid DNA Extraction Kit; Qiagen) and sequenced as described below.

The 241-bp genomic DNA fragment from the affected individual contained amplified products from the normal and mutant alleles. Therefore, a plasmid library was constructed and clones containing the normal and the mutant PCR products were identified by BstnI digestion.

Sequencing of PCR products. For sequencing, amplified PCR products were gel-isolated with QiaxII Gel Extraction Kit (Qiagen). PCR-amplified cDNA, genomic DNA fragments, and plasmid DNA were sequenced on an ABI 373 DNA sequencing system (Perkin-Elmer Corp., Applied Biosystems, Weiterstadt, Germany), using the ABI PRISM Dye Terminatior Cycle Sequencing Kit with Amplitaq DNA Polymerase, FS (Perkin-Elmer Corp., Foster City, CA). 20–40 ng of PCR fragment purified by electrophoresis on agarose gels (10 ng/100-bp fragment length, for sequencing of plasmid DNA 400 ng/reaction), and 3.2 pmol of primer were used in a total volume of 20 μl. The sequencing reactions were performed on a GeneAMP PCR system 2400 (Perkin-Elmer Corp., Applied Biosystems). Cycling parameters were as follows: preheating to 96°C, and then 25 cycles of 30 s at 96°C, 15 s at 50°C, and 4 min at 60°C each. Before loading onto the gel, excess terminators were removed by ethanol precipitation. The reactions were run on a 5.5% polyacrylamide gel (2,550 × 4,000 mm, 3,600 mm WTR) at 32 watts for 11 h.

Protein analysis. Myocardial biopsies were transferred from −80°C directly to SDS-sample buffer with 6 M urea (22), preheated at 90°C, and homogenized. Insoluble material was precipitated and the supernatant analyzed on 14% SDS-polyacrylamide gels (22). For quantitation, gels were stained with Coomassie brilliant blue and the actin band quantified densitometrically with a gel scanner. Samples were adjusted according to equal protein concentrations by appropriate dilution in SDS-sample buffer. Equal volumes were then separated on 8–12% gradient gels and transferred to nitrocellulose membranes (BA85; Schleicher and Schüll, Dassel, Germany) by electroblotting essentially as described (23). Cardiac MyBP-C was detected using the rat polyclonal antibody I1 (18) and a novel rabbit antibody, R76, directed against the recombinant NH_2-terminal modules C1-C2 (I1) or C0-C1 (R76) of human cardiac MyBP-C. Bound antibody was visualized with anti–rat or rabbit horseradish peroxidase conjugate (Sigma Chemical Co., Deisenhofen, Germany) and the ECL-system following the instructions of the supplier (Amersham Life Science). Blots were exposed on X-AR5 film (Eastman Kodak Co., Rochester, NY) between 30 s and 20 min.

For generation of rabbit antiserum R76, the recombinant frag-

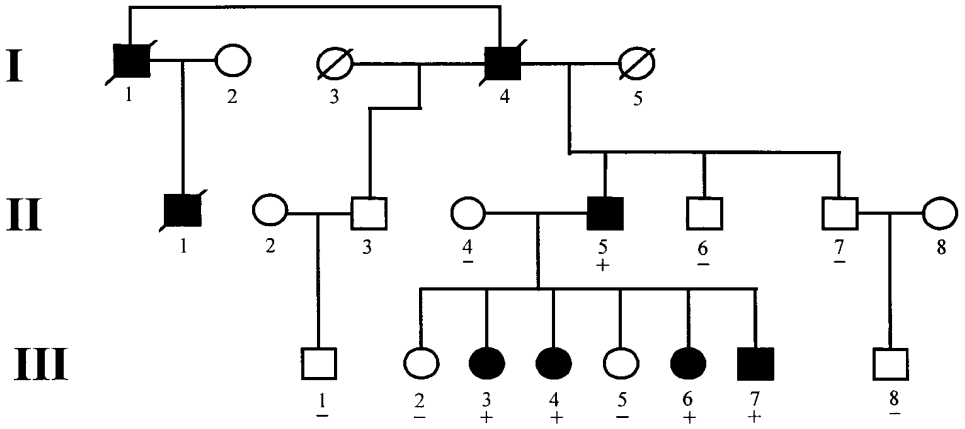

Figure 1. Pedigree of family AY. Symbols denote sex and disease status: box, male; circle, female; darkened, affected; clear, unaffected; slashed, deceased. Genetic affection status is indicated: +, mutation present; −, mutation absent. Individuals identified with +/− were genetically studied.

ment C0-C1 was injected in a standardized scheme using TiterMax adjuvant (CytR Corp., Norcoss, GA). Cardiac-specific reactivity was assayed in immunofluorescence on cardiac and skeletal muscle cryosections and by Western blotting as described (18).

To determine the detection limit of our Western blot, dilution series of the normal heart control were prepared in sample buffer and blotted on 8% gels as described above. The dilution at which the MyBP-C band was still discernible after 2.5-min exposure was defined as the lower detection limit. To prove for incomplete extraction of mutant MyBP-C, precipitated material was assayed after sample buffer extraction by dot blotting in comparison with myofibrils extract.

Results

Clinical evaluation. The clinical investigation of this Caucasian family revealed classical features of FHC (Fig. 1). Three family members had died suddenly at the age of 55, 61, and 50 yr (I-1, I-4, II-1). Individual II-5, the index patient, displayed an interventricular septum thickness of 24 mm on biventricular angiogram (Fig. 2) and echocardiogram. The histopathological examination of his myocardial biopsies showed changes compatible with FHC such as myocyte hypertrophy and disarray. Offspring III-4, III-6, III-7 had an interventricular septum thickness over the 95% prediction limits according to echocardiographic normal values related to age and body surface area (11–13). Individual III-3 was considered affected on a borderline septal wall thickness of 11 mm, clinical symptoms and nonspecific ST-segment, and T-wave changes. All other members of the family had normal clinical findings.

Genetic analysis. Linkage analysis in this family with polymorphic markers excluded cosegregation of FHC with the β-myosin (MYO I, MYO II), α-tropomyosin (D15S108, D15S114), and cardiac troponin T (D1S202, D1S412) genes.

Linkage to cardiac MyBP-C gene on chromosome 11 was tested using flanking markers D11S1344 and D11S1350, which are located in the vicinity of cardiac MyBP-C (8). Both markers showed no recombination in the affected individuals available for genotyping. A maximum two-point logarithm of the odds (LOD) score of 1.25 at $\theta = 0$ was achieved between FHC and D11S1344, and 1.22 at $\theta = 0$ between FHC and the marker D11S1350. A LOD score of 1.94 at $\theta = 0$ was calculated between FHC and the splice donor site mutation in the MyBP-C gene.

RNA and DNA analysis. Lymphocyte mRNA from affected members was amplified by reverse transcription and nested PCR (24–26). Amplification of cardiac MyBP-C cDNA with primers 3300F and 3566R from affected individuals yielded two distinct products: the expected 267-bp product and a 160-bp shorter fragment (Fig. 3). Subcloning and sequencing of the shorter cDNA fragment after gel extraction confirmed the deletion of the 160-bp stretch.

Genomic DNA was amplified with the primer pairs 3300F-3490R and 3445F-3576R to determine whether the aberrant cDNA resulted from a deletion of abnormal splicing. Fig. 4 *A* reveals different SSCP patterns between the affected and healthy individuals when using the primers 3445F and 3576R, but not when genomic primers 3300F and 3490R were used.

Since neither the structure nor the intronic sequences of the cardiac MyBP-C gene were known, we determined the exon–intron boundaries in the region spanning nucleotide positions 3300–3576 by direct sequencing of the genomic PCR product. A 160-bp exon (residues 3363–3522) was identified (Fig. 5). Both a normal intron sequence and a G→A transition were identified in the affected individual at position 1 of the 5′ splice donor sequence gtgct (gtgct→atgct). The G→A transi-

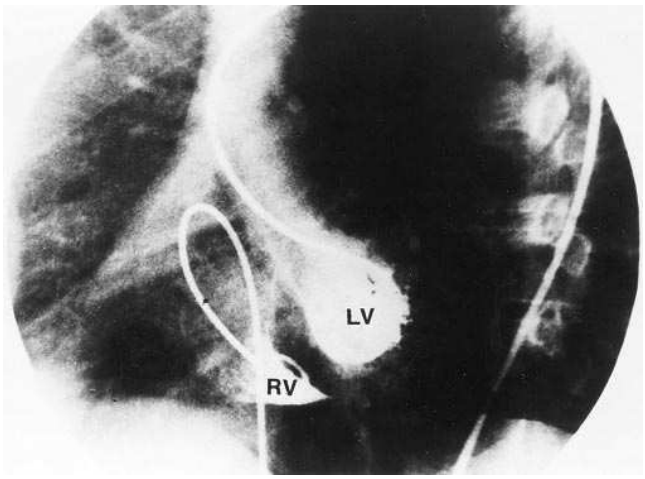

Figure 2. Biventricular angiogram of the index patient. Left ventricular wall thickness was assessed in 30° left anterior oblique projection by simultaneous injection of 30 ml contrast material in both ventricular chambers. LV, left ventricle; RV, right ventricle.

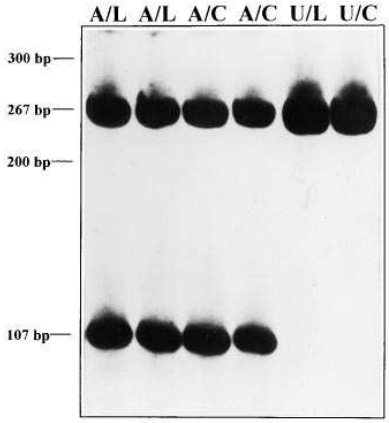

Figure 3. Detection of cardiac MyBP-C splice donor site mutation. Cardiac MyBP-C cDNA amplified from lymphocyte (*L*) and myocardial (*C*) RNA from affected (*A*) and unaffected (*U*) family members using primers 3300F and 3566R. Samples from affected individuals contained the normal 267-bp product and also a 107-bp product resulting from skipping of the 160-bp exon.

tion abolishes a BstnI restriction site, allowing independent confirmation of the mutation either by restriction enzyme digestion or SSCP analysis. BstnI digestion of the 241-bp product between 3445F and 3576R from unaffected individuals showed four fragments of 117, 75, 27, and 22 bp. In contrast, BstnI digestion of the 241-bp product from the index patient and the affected individuals showed an additional fragment of 102 bp (Fig. 4, *B* and *C*). This indicates the presence of both a normal and mutant allele in affected family members. All clinically affected members including the equivocal patient III-3 carried the mutation. The mutation was present in neither the unaffected family members nor 250 unrelated healthy individuals.

mRNA from two different left ventricular endomyocardial biopsies of the index patient (II-5) was reverse transcribed and amplified using primers 3300F and 3566R. Two cDNA products of 267 and 107 nucleotides were found confirming the results obtained from lymphocyte cDNA (Fig. 3). The shorter cDNA fragment also lacked the exonic region between residues 3363 and 3522.

The ratio of the abnormally spliced, shorter cDNA fragment to the wild-type cDNA fragment was determined by film densitometry scanning (20). The signal of lymphocyte and myocardial cDNA amplified from the mutant allele ranged from 85–95% of that observed from the wild-type allele depending on the number of PCR cycles and the exposure time of the blot to the film.

Protein analysis. Western blot analysis for cardiac MyBP-C of four individual biopsies from the index patient was performed and the results compared with reference samples of ventricular tissue from patients with aortic stenosis, ischemic cardiomyopathy, and ventricular septum defect. The Western blot with an antibody directed against the amino-terminal region of cardiac MyBP-C revealed the presence of a single band corresponding to the normal protein in all samples investigated (Fig. 6). In particular, the predicted truncated protein of 124.5 kD derived from translation of the misspliced mRNA of the disease-associated allele could not be detected. Longer exposures of the blot also did not reveal the predicted truncated protein product. To address the possibility that antibody epitopes could be masked in Western blot assay despite the use of denaturing gels and blotting conditions, we assayed biopsies 2 and 3 of the index patient in duplicate with a novel serum (R76), raised against the recombinant fragment C0-C1 of human cardiac MyBP-C. This serum reacted to the same band

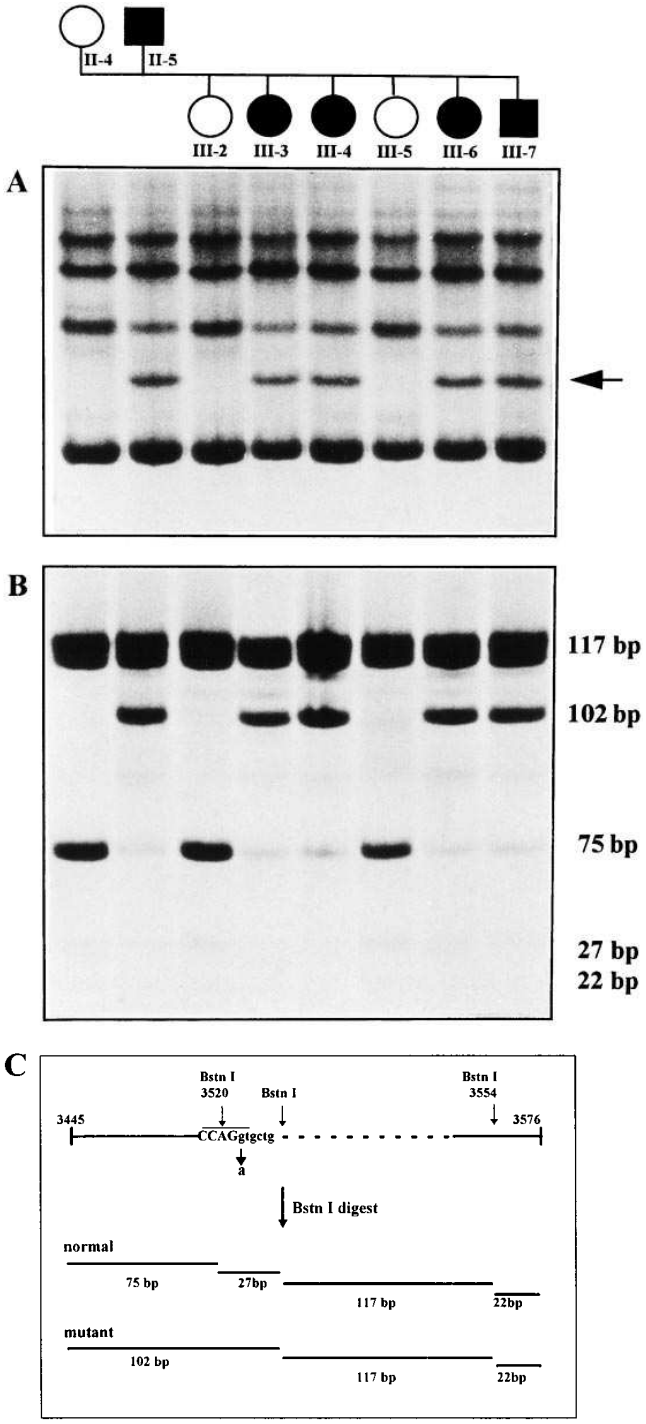

Figure 4. Identification of the point mutation in the cardiac MyBP-C gene. Symbols as in Fig. 1. (*A*) SSCP analysis of genomic PCR fragments generated with 3445F and 3576R primers. Additional band (*arrow*) was observed in affected individuals. (*B*) BstnI enzyme digestion of genomic PCR fragments generated with 3445F and 3576R primers. In the mutant allele, the loss of a BstnI restriction site results in noncleavage of a 102-bp fragment between nucleotide 3445 and the 25th nucleotide of the following intron. Short fragments (27 and 22 bp) are hardly visible on the gel due to their small size. (*C*) BstnI restriction map of PCR fragment generated with 3445F and 3576R. BstnI restriction sites are indicated with arrows and nucleotides are numbered according to the Genbank/EMBL/DDBJ data library (accession No. X84075). The BstnI site, abolished by the splice donor site mutation, is marked with a dash.

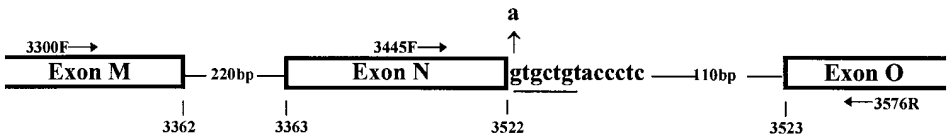

Figure 5. The cardiac MyBP-C gene structure in the region of exon N. Nucleotide residues defining exon–intron boundaries are numbered below; exons are labeled according to Watkins et al. (9). The g→a transversion at position 1 of the 5′ splice donor sequence (*underlined*) is indicated. The mutation abolishes a BstnI restriction site.

in the normal control as the serum I1. In the biopsy specimens, we observed no discernible difference in the band patterns between the sera I1 and R76 (Fig. 7 *A*). Since incomplete extraction of mutant MyBP-C could also explain the lack of immunoreactive material in Western blots, we assayed the residual material after sample buffer extraction by dot blotting in comparison with the total myofibrils extract. Residual material after extraction in sample buffer showed no immunoreactivity with the anti–MyBP-C antibodies I1 and R76 (Fig. 7 *D*). We conclude that MyBP-C can be readily extracted from myocardial tissue using denaturing SDS/urea sample buffer.

The lower detection limit of the Western blot was defined as the dilution at which the MyBP-C band was still discernible. With exposure times of 2.5 min, this limit was 1.5% of the undiluted control (Fig. 7 *C*). We assume, therefore, that mutant protein expressed at levels lower than 1.5% of wild type would not be detectable in our assay. To investigate if lower amounts of wild-type cardiac MyBP-C are expressed in diseased myocardium, the amount of wild-type cardiac MyBP-C in patient II-4 was measured by scanning and normalized to actin (Fig. 7 *B*). The amount of expressed protein appeared normal when compared with unrelated control patients. Therefore, no evidence for a lower expression due to a gene dose effect was found.

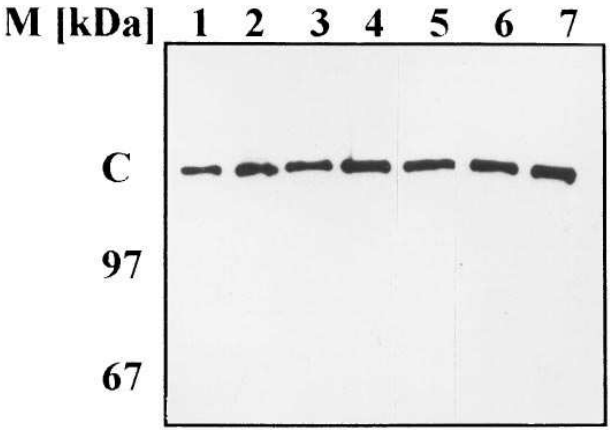

Figure 6. Western blot analyses of myocardial biopsies. Cardiac MyBP-C was detected using the rat polyclonal antibody I1 directed against the recombinant NH_2-terminal modules C1-C2 of human cardiac MyBP-C. Bound antibody was visualized with anti–rat-HRP conjugate and the ECL system. (Lanes *1–4*) Different myocardial biopsies from the index patient. (Lanes *5–7*) Reference samples of ventricular tissue from patients with ischemic cardiomyopathy (lane *5*), aortic stenosis (lane *6*), and ventricular septum defect (lane *7*). C, cardiac MyBP-C.

Discussion

Recent findings defined cardiac MyBP-C mutations as a possible cause of FHC. Based on altered lymphocyte cDNA sequence, the mutations described so far are predicted to produce a truncated cardiac MyBP-C with disruption of the titin and myosin-binding COOH-terminal region (27). Bonne et al. (8) found a splice acceptor mutation of the MyBP-C gene in two unrelated French families, which causes the skipping of the associated exon and could eventually produce truncated cardiac MyBP-C. The mutation described is located in the linker module between immunoglobulin domains C4 and C5 (Fig. 8). Watkins et al. (9) demonstrated a splice donor mutation in the immunoglobulin domain C9 and a duplication mutation in immunoglobulin C10 domain in two families with FHC. Both mutations are predicted to alter the myosin- and titin-binding COOH terminus of cardiac MyBP-C. More recently, six novel mutations in unrelated French families have been identified, all of which were predicted to lead to expression of truncated cardiac MyBP-C (28). However, the transcription of the mutant alleles in cardiac tissue and the fate of the predicted truncated proteins remained unclear.

In this study, we have identified a novel mutation in the cardiac MyBP-C gene from a Turkish family with FHC. The splice donor site mutation in the COOH terminus (immunoglobulin domain C9) was not observed in unaffected family members and controls. The mutation cosegregates with the disease in an autosomal dominant trait. Four endomyocardial biopsies of the index patient were available and analyzed for cardiac MyBP-C mRNA and protein composition. Study of myocardial mRNA revealed two alleles: the normal and a mutated allele with skipping of the associated exon. These findings demonstrate that the mutation is transcribed to mRNA in cardiac tissue. The skipping of exon N (Fig. 5) in cardiac cDNA is a consequence of the G→A transition of the highly conserved position 1 of the 5′ splice donor consensus sequence in the absence of an alternative splice donor site in the following intron (29–31). Skipping of the 160-bp exon N produces a frame shift. The aberrant cDNA encodes for a MyBP-C with 1,025 normal and 24 novel amino acids, followed by a premature termination of translation due to a TAG stop codon. As a consequence, 164 amino acids of the conserved COOH terminus are deleted (Fig. 8) and partially replaced by 24 novel residues, resulting in a mass difference of 16.4 kD. This mass difference is predicted to result in a detectable mobility shift on protein gels. However, Western blot analysis with two different antibodies failed to detect either the truncated protein or a discernible reduction of nontruncated MyBP-C protein concentration compared with sarcomeric actin (Figs. 6 and 7 *A*). The wild type allele of MyBP-C seems to largely compensate

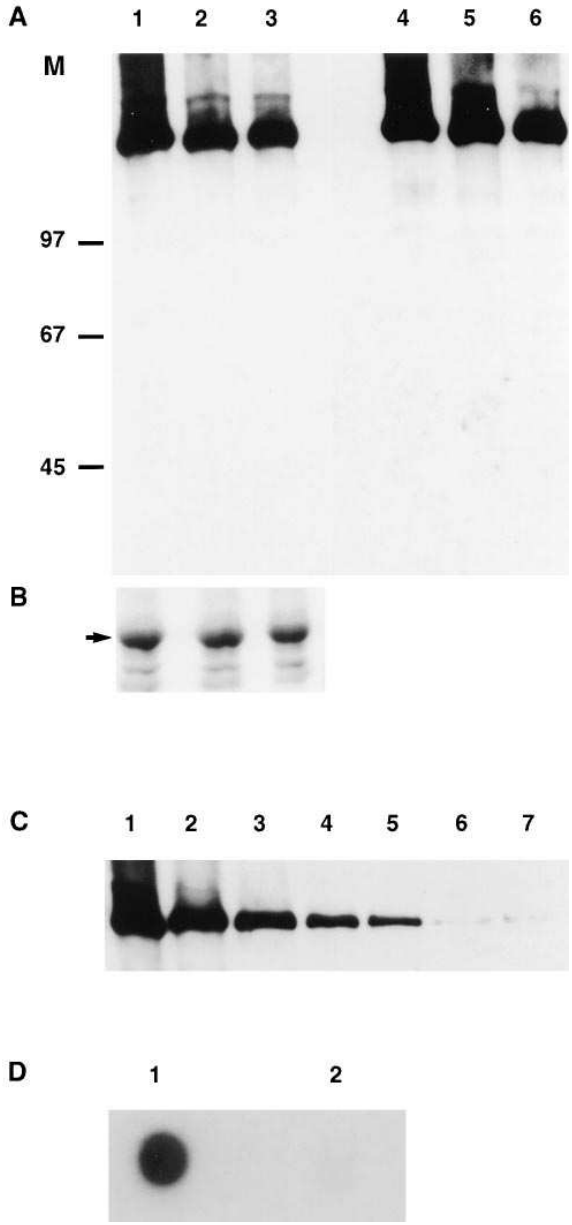

Figure 7. Western blot analysis of myocardial biopsies. (*A*) Western blot analysis of control myocardium (lanes *1* and *4*), and biopsies 2 (lanes *2* and *5*) and 3 (lanes *3* and *6*) using two different polyclonal antibodies against different regions of the cardiac MyBP-C NH_2 terminus. Lanes *1–3*, serum I1 (anti–C1-C2); lanes *4–6*, serum R76 (anti–C0-C1). The blots were loaded at twice the protein load as in Fig. 6 and exposed for up to 6 min. Both antibodies detect the full-length MyBP-C, but no discernible additional bands specific for the biopsy specimens, even at the long exposure times and high protein loading used. (*B*) Control showing the actin band (*arrow*) of a Coomassie-stained gel with replica lanes of *1–3* in *A*. The biopsies (lanes *2* and *3*) show comparable actin bands as the control sample. The MyBP-C signals of the Western blot appears equal compared with the sarcomeric actin bands. (*C*) Dilution series of the normal heart control, probed with antibody I1 for cardiac MyBP-C. Lane *1*, loading as in *A*. The concentration was decreased in steps of twofold (lane *2*, 1/2; lane *3*, 1/4; lane *4*, 1/8; lane *5*, 1/16; lane *6*, 1/32; lane *7*, 1/64). Exposure time of the blot was 2.5 min. Protein amounts corresponding to at least 1.5% of the normal control can be detected. (*D*) Dot blot of SDS extract of biopsy 2 (lane *1*) and the extracted particulate material (lane *2*). Cardiac MyBP-C immunoreactive material was detected with antibody I1; exposure time was 3 min. The SDS extract corresponds to twice the gel loading as in *A*; the residual material was homogenized in 8 M urea corresponding to the volume of the SDS extract (100 μl), and equal volumes were spotted. No immunoreactive material is detectable in the residual pellet of connective tissue, suggesting that MyBP-C can be completely extracted from the biopsy material by SDS/6M urea sample buffer.

for the synthesis of MyBP-C protein in the assembled myofibril.

Nondetection of the mutant MyBP-C due to altered folding of the truncated peptide, and therefore altered exposure of the relevant epitopes in both the regions C0-C1 and C1-C2, seems to be unlikely in denaturing gels. Gilbert et al. (32) transfected skeletal muscle myoblast with expression plasmids encoding truncation mutants of MyBP-C. The truncation mutant Delta D9-10, which is very similar to that produced by the splice donor site mutation described here, could be detected with antibodies directed against the NH_2 terminus of the construct. The truncation mutants of MyBP-C also migrated on SDS-PAGE with the predicted mobility (32). Our Western blot assay showed to be sensitive for small amounts of protein and could detect $\sim$ 1.5% of protein compared with wild-type MyBP-C (Fig. 7 *C*). We cannot, therefore, completely exclude the presence of traces of truncated MyBP-C in myocardial tissue, which might still act as a poison polypeptide. However, even long exposures of the blots did not reveal a band of lower mobility than the wild-type protein, specific for the diseased myocardium (not shown). If truncated cardiac MyBP-C is present at all in the myocardium, its levels are very low. A transgenic mouse model for FHC with cardiac-specific expression of mutant rat alpha myosin heavy chain demonstrated that already low levels of mutant protein, 0.6–12% of the total myosin, in the presence of a normal actin/myosin stoichiometry induces a severe phenotype of FHC. The authors suggested that the severe phenotype is due to the dominant effect of the mutant such that a relatively small number of mutant polypeptides exert a "drag" on sarcomere function (33). However, although the poison peptide hypothesis cannot be totally excluded, as traces of mutant MyBP-C could remain undetected, it is not the necessary and sufficient mechanism for the genesis of FHC by mutations in the cardiac MyBP-C. We propose that the changes of this cardiac MyBP-C mutation must be sought in the assembly of the sarcomere itself rather than in the assembled structure. The absence of detectable amounts of truncated MyBP-C protein despite the presence of the corresponding mRNA transcript is plausibly explained by rapid proteolysis of the nonassembled mutant protein by the proteasome complex of developing muscle (34). The predicted result would be a drastic change of protein stoichiometry during myofibril assembly. Similarly, a rapid degradation of nonassembled, cytosolic troponin T protein was described in a 5′ splice donor site mutation in intron 7 of Drosophila flight muscle troponin T, resulting in the *upheld*^{2} phenotype (35). For mutations in the actin and myosin heavy chain genes of *D. melanogaster*, changes in myofibrillar stoichiometry have been observed to result in altered myofibril turnover and ultimately in myofibril disarray (36). Since cardiac MyBP-C is essential for myofibrillar assembly (27, 37), reduced amounts of functional protein during the assembly process could equally lead to misassembly and sarcomeric disarray, which is the histological hallmark of FHC.

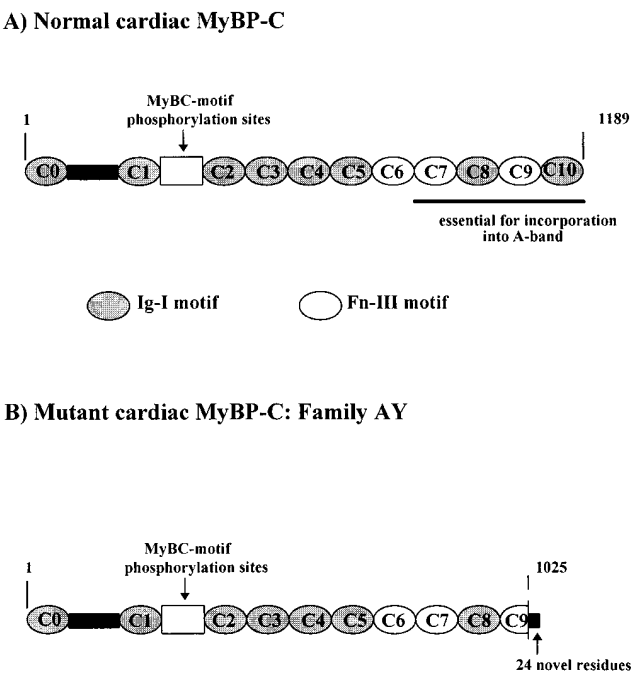

Figure 8. Normal and mutant cardiac MyBP-C polypeptides. (*A*) The normal cardiac MyBP-C is composed of eight immunoglobulin-I motifs, (*Ig-I motif*), three fibronectin type III (*fn-III motif*) repeats, and the cardiac isoform-specific phosphorylation site (*MyBP-C motif*). Amino acid residue numbers are according to the Genbank/EMBL/DDBJ data library (accession No. X84075). The domains essential for incorporation of MyBP-C into A-bands are marked according to Gilbert et al. (38). (*B*) The predicted truncated protein product of the aberrantly spliced MyBP-C cDNA. Skipping of the 160-bp exon N results in loss of the terminal 164 amino acid residues, including the myosin-binding C10 domain; a frameshift encodes 24 novel residues followed by premature termination.

Our study shows that the diseased allele contributes to approximately similar levels of message as the wild-type allele, but does not lead to detectable amounts of the truncated protein. This observation leaves neither the null allele nor the poison peptide hypothesis as the only necessary and sufficient causes for the genesis of FHC by mutations in the cardiac MyBP-C. Possibly, other novel mechanisms are relevant to the development of FHC. In this context, it may be significant that different classes of mutations are typical for genes that are known genetic causes of FHC. For the human cardiac β myosin heavy chain gene, point mutations that locate in the head or head-rod region of the protein are typical (for review see reference 38). The point mutations in the cardiac β myosin heavy chain gene indeed appear to be sufficient for the initiation of FHC as recently confirmed by gene targeting studies in mice (39). In contrast with the human cardiac β myosin heavy chain mutations, none of the identified cardiac MyBP-C mutations (8, 9, 28, and this study) resembles a point mutation. Instead, all 10 mutations are splice donor, splice acceptor, deletion, or insertion mutations. Thereby, all mutations are predicted to lead to an altered mRNA sequence. Possibly, no truncated cardiac MyBP-C expression can be detected despite the presence of mutant transcripts, because MyBP-C translation requires a correctly folded RNA template (for review see reference 40). On the protein level, cardiac MyBP-C is known to bind to titin at multiple and regular intervals (27, 41), which contributes to the formation of highly ordered and stable thick filaments (32). The translation and the assembly of titin and MyBP-C into sarcomeres are possibly coregulated and interdependent. This may involve colocalization of the respective mRNAs to spatially coordinate the assembly (42). Possibly, a mutant cardiac MyBP-C transcript might therefore interfere with the formation of ordered sarcomeres already on the mRNA level. Such a scenario could explain why, so far, all known mutations in the cardiac MyBP-C gene significantly affect the transcript sequence by splice donor, splice acceptor, or duplication mutations, and therefore presumably its folded structure.

Two previous studies have described the effects of COOH-terminally truncated MyBP-C transfected into vertebrate myocytes (32, 43). These experiments, especially the detailed study by Gilbert et al. (32), highlighted the complex interactions in the COOH terminus of MyBP-C involved in sarcomere assembly. It was demonstrated that the COOH-terminal Ig domain is essential for thick-filament targeting. Domains C8–C10 are minimal requirements for A-band incorporation. The lack of domains C10 and/or C9 causes myofibrillar disarray only in the presence of domain C8, while these constructs are not incorporated into the A-band in detectable amounts. In contrast, COOH-terminally truncated constructs shorter than domain C8 were neither dominant negative nor localized to the A-band. Additional protein interactions, localized in the region that binds to titin in vitro (27, 32), appear to be crucial for correct sarcomeric assembly. The observed myofibrillar disarray thus seems to be caused by competition of truncated MyBP-C with A-band components, most likely titin. However, the transfection studies in cell culture with forced overexpression of mutated protein under control of strong viral promoters resulted in the rapid disturbance of sarcomere assembly (32, 43), which contrasts with the late manifestation of FHC in family members carrying the mutation and with the rather slow progression of the disease in clinically affected patients. Furthermore, the splice acceptor mutation of MyBP-C described by Bonne et al. (8) is predicted to produce a truncated protein, which is lacking the domains C5–C10. The transfection studies by Gilbert et al. (32) did not reveal any significant dominant negative effect on myofibrillar assembly for the similar construct D7-10. Therefore, cell culture models and transfection assays may not reflect the assembly control of myofibrillar proteins in the diseased myocardium and therefore the pathogenesis of chromosome-11–associated FHC.

In conclusion, the common denominator of all MyBP-C mutant proteins known to date is the loss of their thick-filament targeting region in domains C8–C10 by a variety of different and unrelated mutation mechanisms, either in the coding exons themselves or acting on transcript processing. Our results suggest that the truncated unassembled polypeptide is rapidly degraded. We propose, therefore, that disturbance of the dynamic process of myofibrillar assembly by altered protein stoichiometry may be the most plausible cause for the resulting disarray. Clearly, a better understanding of the causal mechanisms that translate the mutations of the MyBP-C to the clinical phenotype will require further analysis of possible interactions of both the mutated MyBP-C protein and the transcript in vitro and the evaluation of their long term consequences in the afflicted myocardium in transgenic animals.

Acknowledgments

We are indebted to the family members for their invaluable participation. We are also grateful to E. Rodemer for assistance with collection of clinical data and blood samples, to M. Rittirsch and A. Kempkes for technical assistance, and to G. Kunst and C. Vahl for samples of reference myocardium.

This work was supported by DFG-grant 405/3-1 (M. Gautel) and 368/1-1(Ze).

References

1. Maron, B.J., R.O. Bonow, R.O. Cannon, M.B. Leon, and S.E. Epstein. 1987. Hypertrophic cardiomyopathy: interrelations of clinical manifestations, pathophysiology, and therapy. *N. Engl. J. Med.* 316:780–789 and 844–852.

2. Jarcho, J. A., W. McKenna, J.A. Pare, S.D. Solomon, R.F. Holocombe, S. Dickie, T. Levi, H. Donis-Keller, J.G. Seidman, and C.E. Seidman. 1989. Mapping a gene for familial hypertrophic cardiomyopathy to chromosome 14qI. *N. Engl. J. Med.* 321:1372–1378.

3. Geisterfer-Lowrance, A.A., S. Kass, G. Tanigawa, H.-P. Vosberg, W. McKenna, C.E. Seidman, and J.G. Seidman. 1990. A molecular basis for familial hypertrophic cardiomyopathy: a beta-cardiac myosin heavy chain gene missense mutation. *Cell.* 62:999–1006.

4. Thierfelder, L.C., C. MacRae, H. Watkins, J. Tomfohrde, W. McKenna, K. Bom, G. Noeske, M. Schlepper, J. Just, A. Bowcock, et al. 1993. A familial hypertrophic cardiomyopathy locus maps to chromosome 15q2. *Proc. Natl. Acad. Sci. USA*. 90:6270–6274.

5. Thierfelder, L.C., H. Watkins, C. MacRae, R. Lamas, W. McKenna, H.P. Vosberg, J.G. Seidman, and C.E. Seidman. 1994. α-Tropomyosin and cardiac troponin T mutations cause familial hypertrophic cardiomyopathy: a disease of the sarcomere. *Cell*. 77:701–712.

6. Watkins, H., C. MacRae, L. Thierfelder, Y. Chou, M.P. Frenneaux, W. McKenna, J.G. Seidmann, and C.E. Seidman. 1993. A disease locus for familial hypertrophic cardiomyopathy maps to chromosome 1q3. *Nat. Genet.* 3:333–337.

7. Carrier, L., J. Hengstenberg, J.S. Beckmann, P. Guicheney, C. Dufour, J. Bervovici, E. Dausse, I. Berebbi-Bertrand, C. Wisnewski, D. Pulvenis, et al. 1993. Mapping of a novel gene for familial hypertrophic cardiomyopathy to chromosome 11. *Nat. Genet.* 4:311–313.

8. Bonne, G., L. Carrier, J. Bercovici, C. Cruaud, P. Richard, B. Hainque, M. Gautel, S. Labeit, M. James, J. Beckmann, et al. 1995. Cardiac myosin binding protein-C gene splice acceptor site mutation is associated with familial hypertrophic cardiomyopathy. *Nat. Genet.* 11:438–440.

9. Watkins, H.,D. Conner, L. Thierfelder, J.A. Jarcho, C. MacRae, W. McKenna, B.J. Maron, J.G. Seidman, and C.E. Seidman. 1995. Mutations in the cardiac myosin binding protein-C gene on chromosome 11 cause familial hypertrophic cardiomyopathy. *Nat. Genet.* 11:434–437.

10. McRae, C.A., N. Ghaisas, S. Kass, S. Donnelly, C.T. Basson, H.C. Watkins, R. Anan, L.H. Thierfelder, K. McGarry, E. Rowland, et al. 1995. Familial hypertrophic cardiomyopathy with Wolff-Parkinson White syndrome maps to a locus on chromosome 7q3. *J. Clin. Invest.* 96:1216–1220.

11. Henry, W.L., J. Ware, J.M. Gardin, S.I. Hepner, J. McKay, and M. Weiner. 1978. Echocardiographic measurements in normal subjects: growth-related changes that occur between infancy and early adulthood. *Circulation.* 57:278–285.

12. Gardin, J.M., W.L. Henry, D.D. Savage, J.H. Ware, C. Burns, and J.S. Borer. 1979. Echocardiographic measurements in normal subjects: evaluation of an adult population without clinically apparent heart disease. *JCU (J. Clin. Ultrasound)*. 7:439–447.

13. Goldberg, S.J., H.D. Allen, and D.J. Sahn. 1975. Pediatric and adolescent echocardiography. Yearbook Medical Publishers, Chicago. pp. 309–314.

14. Gyapay, G., J. Morissette, A. Vignal, C. Dib, C. Fizames, P. Millasseau, S. Marc, G. Bernardi, M. Lathrop, and J. Weissenbach. 1994. The 1993-1994 Genethon human genetic linkage map. *Nat. Genet.* 7:246–339.

15. Vignal, A. 1993. Nonradioactive multiplex procedure for genotyping of microsatellite markers. *In* Methods in Molecular Genetics: Chromosome and Gene Analysis 1. K.W. Adolph, editor. Academic Press Inc., Orlando, FL. pp. 211–221.

16. Lathrop, G.M., J.M. Lalouel, C. Julier, and J. Ott. 1984. Strategies for multilocus linkage analysis in humans. *Proc. Natl. Acad. Sci. USA.* 81:3443–3446.

17. Chergwin, J.M., A.E. Przybyla, R.J. MacDonald, and W.J. Rutter. 1979. Isolation of biology active ribonucleic acid from sources enriched in ribonuclease. *Biochemistry*. 18:5274–5299.

18. Gautel, M., O. Zuffardi, A. Freiburg, and S. Labeit. 1995. Phosphorylation switches specific for the cardiac isoform of myosin binding protein-C: a modulator of cardiac contraction? *EMBO (Eur. Mol. Biol. Organ.). J.* 14:1952–1960.

19. Southern, E.M. 1975. Detection of specific sequences among DNA fragments separated by gel electrophoresis. *J. Mol. Biol.* 98:503–517.

20. Crotty, P.L., R.A. Staggs, P.T. Porter, A.A. Killeen, and R.C. McGlennen. 1994. Quantitative analysis in molecular diagnostics. *Hum. Pathol.* 25:572–579.

21. Bassam, B.J., G. Caetano-Anolles, and P.M. Gresshoff. 1991. Fast and sensitive silver staining of DNA in polyacrylamide gels. *Anal. Biochem.* 196:80–83.

22. Laemmli, U.K. 1970. Cleavage of structural proteins during the assembly of the head of bacteriophage T4. *Nature (Lond.).* 227:680–685.

23. Towbin, H., T. Staehlin, and J. Gordon. 1979. Electrophoretic transfer of proteins from polyacrylamide gels to nitrocellulose sheets: procedure and some applications. *Proc. Natl. Acad. Sci. USA.* 76:4350–4354.

24. Watkins, H., W.J. McKenna, L. Thierfelder, H.J. Suk, R. Anan, A. O'Donoghue, P. Spirito, A. Matsumori, C.S. Moravec, J.G. Seidman, and C.E. Seidman. 1995. The role of mutations in cardiac troponin T and α-tropomyosin in familial hypertrophic cardiomyopathy. *N. Engl. J. Med.* 332:1058–1064.

25. Rosenzweig, A., H. Watkins, D.-S. Hwang, M. Miri, W. McKenna, T. Traill, J.G. Seidman, and C.E. Seidman. 1991. Preclinical diagnosis of familial hypertrophic cardiomyopathy by genetic analysis of blood lymphocytes. *N. Engl. J. Med.* 325:1753–1760.

26. Sarker, B., and S. Sommer. 1989. Access to a messenger RNA sequence or its protein product is not limited by tissue or species specificity. *Science (Wash. DC).* 244:331–334.

27. Freiburg, A., and M. Gautel. 1996. A molecular map of the interactions between titin and myosin-binding protein C. Implications for sarcomeric assembly in familial hypertrophic cardiomyopathy. *Eur. J. Biochem.* 235:317–323.

28. Carrier, L., G. Bonne, E. Baehrend, B. Yu, P. Richard, F. Niel, B. Hainque, C. Cruaud, F. Gary, S. Labeit, et al. 1997. Organization and sequence of human cardiac myosin binding protein C gene (MYBPC3) and identification of mutations predicted to produce truncated proteins in familial hypertrophic cardiomyopathy. *Circ. Res.* 80:427–434.

29. Shapiro, M.B., and P. Senapathy. 1987. RNA splice junctions of different classes of eukaryotes: sequence statistics and functional implications in gene expression. *Nucleic Acids Res.* 15:7155–7174.

30. Green, M.R. 1986. Pre-mRNA splicing. A. *Rev. Genet.* 20:671–708.

31. Robberson, B.L., G.J. Cote, and S.M. Berget. 1990. Exon definition may facilitate splice site selection in RNAs with multiple exons. *Mol. Cell. Biol.* 10: 84–94.

32. Gilbert, R., M.G. Kelly, T. Mikawa, and D.A. Fischman. 1996. The carboxyl terminus of myosin binding protein C (MyBP-C, C-protein) specifies incorporation into the A-band of striated muscle. *J. Cell Sci.* 109:101–111.

33. Vikstrom, K.L., S.M. Factor, and L.A. Leinwand. 1996. Mice expressing mutant myosin heavy chains are a model for familial hypertrophic cardiomyopathy. *Mol. Med.* 2:556–567.

34. Tanaka, K., T. Tamura, T. Yoshimura, and A. Ichihara. 1992. Proteasomes. Protein and gene structures, *New Biol.* 4:173–187.

35. Fyrberg, E., C.C. Fyrberg, C. Beall, and D.L. Saville. 1990. Drosophila melanogaster troponin-T mutations engender three distinct syndromes of myofibrillar abnormalities. *J. Mol. Biol.* 216:657–675.

36. Beal, C.J., M.A. Sepanski, and E.A. Fyrberg. 1989. Genetic dissection of Drosophilia myofibril formation: effects of actin and myosin heavy chain null alleles. *Genes Dev.* 3:131–140.

37. Fürst, D.O., and M. Gaurtel. 1995. The anatomy of a molecular giant: how the sarcomeric cytoskeleton is assembled from molecules of the immunoglobulin superfamily. *J. Mol. Cell. Cardiol.* 27:951–959.

38. Vikstrom, K.L., and L.A. Leinwand. 1996. Contractile protein mutations and heart disease. *Curr. Opin. Cell Biol.* 8:97–105.

39. Geisterfer-Lowrance, A.A., M. Christe, D.A. Conner, J.S. Ingwall, F.J. Schoen, C.E. Seidman, and J.G. Seidman. 1996. A mouse model of familial hypertrophic cardiomyopathy. *Science (Wash. DC)*. 272:731–734.

40. Brown, E.J., and S.L. Schreiber. 1996. A signaling pathway to translational control. *Cell*. 86:517–520.

41. Labeit, S., and B. Kolmerer. 1995. Titins, giant proteins in charge of muscle ultrastructure and elasticity. *Science (Wash. DC).* 270:293–296.

42. Fulton, A.B., and T.L'Ecuyer. 1993. Cotranslational assembly of some cytoskeletal proteins: implications and prospects. *J. Cell Sci.* 105:867–871.

43. Koshida, S., M. Kurasawa, M. Yasuda, N. Sato, and T. Obinata. 1995. Assembly of cardiac C-protein during myofibrillogenesis in myogenic cells in culture. *Cell Struct. Funct.* 20:253–261.